

# The Early Age Behavior of Biomass Fired and Co-fired Fly Ash in Concrete

**Christopher R. Shearer<sup>1</sup>, Nortey Yeboah<sup>1</sup>, Kimberly E. Kurtis<sup>1</sup> and Susan E. Burns<sup>1</sup>**

<sup>1</sup>School of Civil and Environmental Engineering, Georgia Institute of Technology, 790 Atlantic Dr., Atlanta, GA 30332-0355, USA

KEYWORDS: biomass, fly ash, concrete, hydration, workability

## ABSTRACT

The combustion of biomass (e.g., trees, switchgrass) and the co-combustion of biomass with coal can be sustainable energy sources and reduce carbon dioxide emissions. The by-products of these processes (biomass and co-fired fly ash, respectively) are not addressed in U.S. standards for fly ash use in concrete; however, recent European standards have permitted co-fired fly ash use with certain restrictions. The engineering properties of biomass and co-fired fly ash are relatively unknown compared to coal fly ash. This study characterizes the effect of five of these ashes on early age behavior of concrete. Isothermal calorimetry is utilized to analyze early age hydration kinetics. Preliminary testing indicates that the substitution of cement with both ash types at 25% by mass decreases hydration heat, as expected, but with co-fired fly ash exhibiting slightly higher hydration heat than coal fly ash. Furthermore, the biomass fly ash examined significantly increases the tricalcium aluminate hydration peak. The influence of biomass and co-fired fly ash on workability and setting time is also analyzed. The observed behaviors are then linked to the chemical and physical properties of the ashes evaluated through advanced analytical techniques (i.e., XRF, SEM, XRD, etc.). Microscopy has revealed that biomass and co-fired fly ash morphology can be different than coal fly ash. Therefore, it is necessary to assess the impact of this emerging class of energy by-products on concrete performance before they become a viable supplementary cementitious material.

## INTRODUCTION

Fly ash is a finely divided solid aluminosilicate by-product of the coal combustion process that can be utilized in many applications. In 2009, the American Coal Ash Association estimated that nearly 40% of the 63 million tons of coal fly ash generated in the U.S. were beneficially used.<sup>1</sup> Yet there is another emerging class of energy by-products that may also have desirable properties for beneficial reuse. These by-products are derived from the combustion of biomass and the co-combustion of biomass with coal—called biomass and co-fired fly ash, respectively. These sources of energy can be considered sustainable when the consumption of the biomass is less than its rate of growth<sup>2</sup> and if the biomass intakes more CO<sub>2</sub> during its lifetime than is released during firing.<sup>3</sup> New federal legislation imposing renewable energy requirements

and greenhouse gas emission limits will result in increased biomass and co-fired fly ash production. However, the engineering properties and possible pathways for utilization of these by-products have not been well-examined.

Nearly 50% of the coal fly ash produced in 2009 was used as a supplementary cementitious material (SCM) to partially replace the cement binder—a practice that improves later strength and decreases permeability in concrete. As a pozzolan, calcium hydroxide can be consumed to produce strength-providing calcium silicate hydrates, densifying the ITZ (interfacial transition zone) at the cement-aggregate interface, and refining the concrete microstructure.<sup>4</sup> However, biomass and co-fired fly ash are not addressed in ASTM C 618, which currently defines fly ash as “the finely divided residue that results from the combustion of ground or powdered coal and that is transported by flue gasses”.<sup>5</sup> Studies have shown that wood ash can be used to generate controlled low-strength materials<sup>6</sup> and that co-fired fly ash can perform satisfactorily compared to coal fly ash in concrete with respect to strength and durability.<sup>7-11</sup> Additionally, the current European standard for fly ash use in concrete (EN450-1) permits ashes that are “produced when small quantities of secondary materials are combusted with at least 80% of coal by dry mass in a power station with a maximum ash content of 10% being derived from the secondary material”.<sup>12</sup>

Yet, the inherent variability of fly ash can present challenges in the prediction and control of concrete behavior. The variation in biomass sources can further alter the structure and composition of the ash. Therefore research at a regional level is imperative to determine the effect that co-fired and biomass ash have on concrete. This paper examines the effect of biomass and co-fired ash on the early-age properties of concrete—a topic that has been minimally researched. Fresh concrete properties significantly impact construction practices and have important implications for long-term strength and durability. In this paper the hydration kinetics of ash-cement pastes are recorded utilizing a calorimeter. Furthermore, workability is measured as a function of ash-cement mortar flow and setting times of ash-cement pastes are measured using the Vicat apparatus. The observed behaviors are then linked to the chemical and physical properties of the ashes evaluated through advanced analytical techniques (i.e., XRF, SEM, XRD, etc.). The objective of this study is to determine the capability of biomass and co-fired fly ash used as a SCM in concrete focusing on its effect on plastic properties.

## EXPERIMENTAL

### *Materials*

Ash samples derived from coal combustion, co-firing, and biomass combustion were utilized for this research. A commercially available coal Class F fly ash from Southern Company’s Plant Bowen in Cartersville, GA (CA) was used as a baseline comparison. One coal fly ash sample and two companion co-fired ash samples were produced at Southern Company’s Ernest C. Gaston Electric Generating Plant in Wilsonville, AL (EC). The co-fired samples were generated by firing eastern bituminous coal with wood chips (containing no limbs and minimal bark) with the properties shown in Table 1. The

wood chips and coal were mixed on a belt with two separate reclaim hoppers and crushed with a Babcock & Wilcox EL-76 pulverizer prior to combustion in a 250 MW opposed wall fired burner. In addition, one biomass ash (BA) sample provided by the McNeil Generating Station located in Burlington, Vermont was investigated. The BA sample was produced by firing a mixture of forest residue (i.e., tree limbs) and mill residue (i.e., sawdust). The coal (CA) and biomass (BA) ashes were also mixed to simulate co-fired ash produced at biomass co-firing percentages higher than is capable with current facilities in the Southeast. Data collected from various co-firing tests have shown that the ash contents of local wood range from 0.25-1% while the ash contents of local coal range from 5-15%. Thus blends were produced utilizing the assumption that 100 kg. of wood will produce 1 kg. of wood ash, and 100 kg. of coal will produce 10 kg. of coal ash as seen in Table 2. Additionally, one blend was made for comparison with the EC3 co-fired ash. All testing used commercially available Type I Portland cement (ASTM C 150).<sup>13</sup>

An oxide analysis was performed on the ash samples and cement using X-ray fluorescence spectroscopy as shown in Table 3. Thermogravimetric analysis, which measures the mass loss of a material up to 950°C, was used to determine loss on ignition (LOI). Typically, LOI represents the unburned carbon content of the ash, however it should be noted that nearly half of the LOI for the biomass ash consists of the decomposition of carbonates (primarily calcium and potassium). The surface area and porosity of the CA and BA samples were measured through N<sub>2</sub> gas adsorption isotherms obtained from a Micromeritics TriStar II 3020 system. Brunauer, Emmet, and Teller (BET) theory was used for calculating surface areas. The particle size distributions of the materials are shown in Fig. 1. Size distributions of the ash were measured by laser particle size analysis with dry dispersion, which accommodates particles from 1- 192µm. The agglomeration and angular shape of the BA particles prohibited its use in the laser analyzer. The scanning electron microscopy (SEM) image seen in Fig. 2 reveals the unique morphology of BA compared to the typical spherical morphology of coal-derived fly ash. The long, fibrous wood particles of BA are clearly visible, indicating a possible lack of complete firing. Fig. 3 shows a similar woody particle in the EC2 ash intermixed with the glass spheres demonstrating that co-firing does affect ash morphology.

Table 1: Biomass Properties of EC-Series Ash

Material	FA Type	Wood Properties, %			Wood Type
		Weight	Energy <sup>a</sup>	Moisture <sup>b</sup>	
EC1	Coal Only	-	-	-	-
EC2	Co-Fire	4.0	1.14	49.20	10 mm Pine Chips
EC3	Co-Fire	8.2	3.17	48.06	10 mm Pine Chips

<sup>a</sup>As percent of total BTUs produced during co-firing with coal

<sup>b</sup>Moisture content before co-firing with coal

Table 2: Blending of Coal Ash (CA) and Biomass Ash (BA)

Blends	Wood Ash Yield, <sup>a</sup> kg.	Coal Ash Yield, <sup>a</sup> kg.	Actual Wood Ash %	Actual Coal Ash %
EC3, 8.2% (BL1)	0.08	9.18	0.89	99.11
25% Wood Blend (BL2)	0.25	7.50	3.23	96.77
50% Wood Blend (BL3)	0.50	5.00	9.09	90.91

<sup>a</sup>Assuming 100kg. of combined total fuel is combusted

Table 3: Properties of Ash Samples and Cement

Value, %	CA	EC1	EC2	EC3	BA	Cement <sup>a</sup>
SiO <sub>2</sub>	55.28	42.77	42.84	43.95	7.38	20.45
Al <sub>2</sub> O <sub>3</sub>	27.21	25.62	26.21	26.45	1.16	4.70
Fe <sub>2</sub> O <sub>3</sub>	7.98	14.67	13.87	13.18	0.57	3.32
Σ(SiO <sub>2</sub> +Al <sub>2</sub> O <sub>3</sub> +Fe <sub>2</sub> O <sub>3</sub> )	90.47	83.07	82.92	83.58	9.11	28.47
CaO	1.26	3.83	4.01	3.76	28.29	63.06
MgO	1.23	1.27	1.25	1.25	2.89	3.27
SO <sub>3</sub>	0.07	0.48	0.44	0.52	1.92	2.8
Na <sub>2</sub> O	0.47	0.51	0.52	0.53	0.48	0.07
K <sub>2</sub> O	3.02	2.13	2.08	2.09	5.86	0.53
Na <sub>2</sub> O <sub>eq</sub>	2.46	1.91	1.89	1.91	4.34	0.42
P <sub>2</sub> O <sub>5</sub>	0.19	0.59	0.65	0.65	2.18	0.06
TiO <sub>2</sub>	1.41	1.26	1.31	1.31	0.09	0.25
Mn <sub>2</sub> O <sub>3</sub>	0.06	0.06	0.06	0.06	1.03	0.16
Cr <sub>2</sub> O <sub>3</sub>	0.05	0.07	0.06	0.06	0.00	0.02
ZnO	0.01	0.01	0.01	0.01	0.10	0.06
V <sub>2</sub> O <sub>5</sub>	0.07	0.08	0.08	0.07	-	-
ZrO <sub>2</sub>	0.05	0.07	0.07	0.07	-	-
LOI	1.39	5.87	5.47	5.23	47.96	1.27
Surface Area (m <sup>2</sup> /g)	1.05	-	-	-	10.15	-
Median Particle Size (μm)	16.15	29.91	26.88	23.26	-	10.08

<sup>a</sup>Bogue Potential Composition: 54.00% C<sub>3</sub>S, 15.82% C<sub>2</sub>S, 6.84% C<sub>3</sub>A, 10.10% C<sub>4</sub>AF

The results indicate that the CA and EC1-3 samples can be classified as Class F fly ash under ASTM C 618 chemical requirements, because these ashes meet all of the stipulations including: (1) primary oxides greater than 70%; (2) sulfur trioxide levels less than 5%; (3) moisture contents less than 3%; and (4) loss on ignition less than 6% by weight. None of these properties appear to be correlated with biomass co-combustion

levels with regard to these ashes. The BA sample has a high percentage of volatile matter as indicated by the high LOI, which may be related to poor firing conditions. For example, if the raw biomass has a high moisture content it will reduce the maximum combustion temperature resulting in incomplete combustion.<sup>14</sup> Furthermore, the BA sample has a high alkali content expressed as total soda equivalent, a commonly observed phenomenon with biomass ash due to the more alkaline nature of biomass fuel compared to coal.<sup>15</sup> The BA sample has a low primary oxide content, but consequently its total calcium content is high. X-ray diffraction (XRD) of the BA sample reveals that calcite is the only crystalline component to which the calcium is bound. Moreover, there is no visible amorphous hump, typically located around 15–40° on the 2θ scale, indicating an insignificant glassy phase and weak pozzolanic properties. Conversely, XRD of the co-fired samples shows a pronounced glassy component in addition to multiple crystalline phases including quartz, mullite, hematite, and magnetite—all commonly seen in low-calcium coal fly ash.<sup>16</sup> Misra et al.<sup>17</sup> has shown that calcium carbonate in a variety of wood ashes transforms to CaO at firing temperature greater than 1300°C. Thus it may be possible to thermally treat the BA sample to create more hydraulically reactive crystalline forms of CaO.

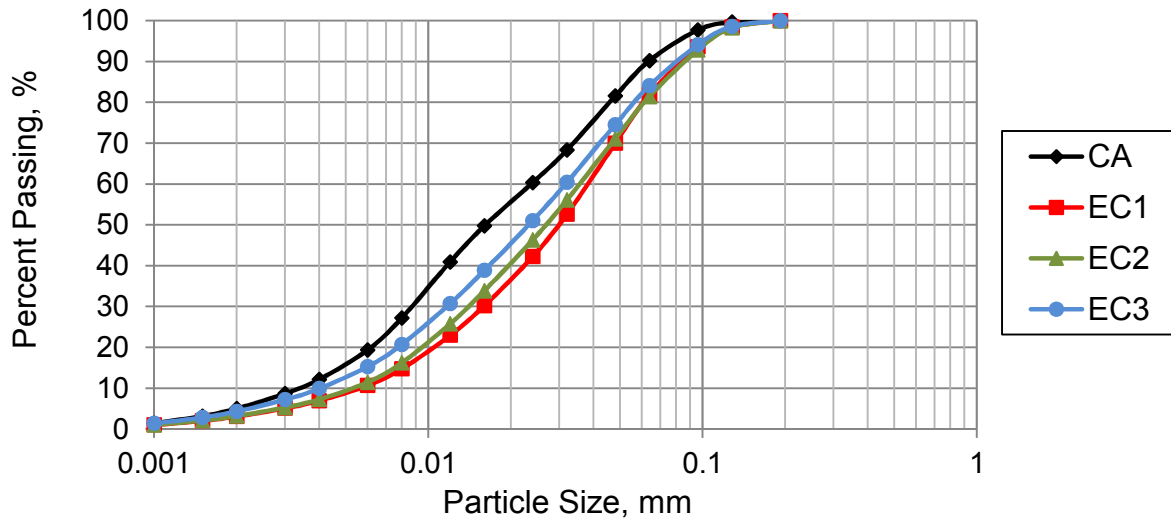


Figure 1: Particle size distribution for ash samples

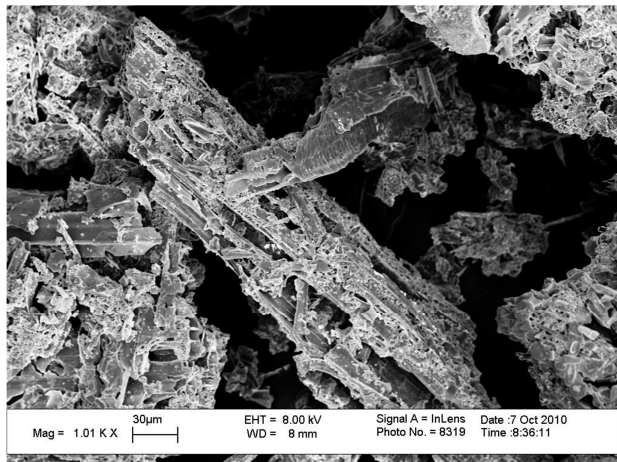


Figure 2: SEM image of biomass ash (BA)

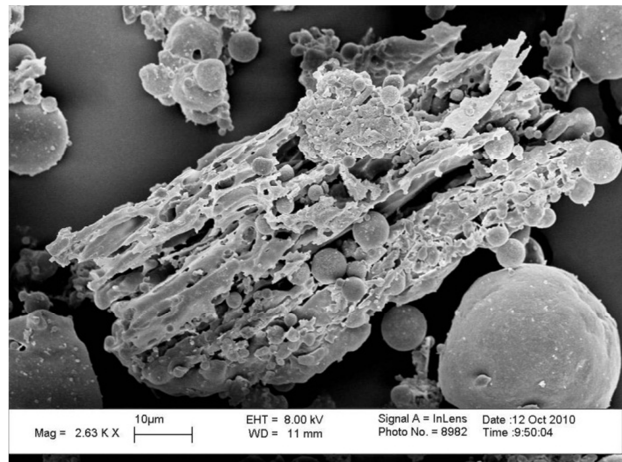


Figure 3: SEM image of co-fired ash (EC2)

### *Isothermal Calorimetry*

Calorimetry was performed on plain cement pastes and binary blends (cement partially replaced with ash). The heat of hydration of the control and binary blends was measured by isothermal calorimetry using a commercial calorimeter maintained at 25°C. ASTM C 1679<sup>18</sup> and mixing methodologies from literature<sup>19</sup> were utilized to produce consistent experimental results. One ash replacement (25% the weight of cement) was used to develop the binary blend pastes. All ash and cement samples were passed through a No. 30 sieve (0.6mm opening) to remove large clumps. Furthermore, the BA sample was oven-dried due to its high (i.e., nearly 50%) in situ moisture content. The water to cementitious material ratio was 0.40 for all mixes. Pastes composed of 100g of total cementitious materials were prepared with a hand mixer. Polyethylene ampoules were filled with 6-7g of paste, while empty ampoules provided a baseline. Each test was performed in duplicate to verify results and data was collected for 48 hours.

### *Mortar flow and Setting Time*

Mortars were produced using the material proportions given for mortar cube strength activity measurements (ASTM C 109)<sup>20</sup>: one part of cement to 2.75 parts fine aggregate and a water to cementitious ratio of 0.485. Ottawa 20-30 sand conforming to ASTM C 778<sup>21</sup> was used as the fine aggregate. One ash replacement (25% the weight of cement) was used to develop the binary blend mortars. Once again, all ash and cement samples were passed through a No. 30 sieve. Mortars were mixed following the procedure provided in ASTM C 305.<sup>22</sup> As described in ASTM C 1437<sup>23</sup>, a conical mold sitting on the flow table was filled with mortar. Then the mold was removed and the table was dropped 25 times in 15 seconds. The flow was measured as the resulting increase in the average diameter of the mortar calculated as a percentage of the original mold base diameter.

The Vicat apparatus was used to measure the time of setting of plain cement pastes and binary blends following the procedure provided in ASTM C 191.<sup>24</sup> One ash replacement (25% the weight of cement) was used to develop the binary blend pastes. The water to cementitious material ratio was 0.35 for all mixes to induce setting at a reasonable time. Initial set was measured as the time between initial mixing and when the Vicat needle penetrated 25mm into the paste. Final set was measured as the time between initial mixing and when the Vicat needle could not penetrate the paste.

## RESULTS AND DISCUSSION

### *Heat of Hydration*

Fig. 4 shows the rate of heat evolution and the cumulative heat evolved for all mixes. Values for both are normalized per gram of cementitious material (i.e., mass of cement and ash). As expected, all of the mixes incorporating 25% ash replacement generated less heat than the control mix—a 19% reduction of cumulative heat evolved on average. The ash decreased the heat of hydration primarily due to the dilution effect as reported in previous studies.<sup>19,25</sup> This phenomenon occurs when less cement (which is highly exothermic) is available for hydration due to the pozzolanic substitution. Two peaks, the

first correlating to the hydration of  $C_3S$  and the second to the hydration of  $C_3A$ , are present on all heat evolution curves. The CA and EC-series mixes retarded these two peaks by 5-25 minutes. The height of both peaks in the EC-series curves appear to be correlated to particle size—with the smallest median particle size (EC3) exhibiting the highest peaks. This trend continues with the CA sample, which is even finer, intensifying the  $C_3A$  hydration more than any EC ash. Yet, the cumulative heat values at 24 hours are slightly higher for the EC-series compared to CA.

Although the EC3 blend (BL1) appears to represent the actual EC3 ash somewhat well in terms of the calorimetry curve, it is apparent that even small additions of BA to CA affect early age hydration in multiple ways. First, for the 25% and 50% co-fired blends (BL2 and BL3, respectively) the dormancy or induction period observed after the initial spike in heat generation is extended by more than 1 hour compared to plain cement and by approximately 50 minutes compared to CA alone. In addition, there is a nearly linear correlation between the BA addition amount and the intensification of the  $C_3A$  hydration. The  $C_3S$  hydration is also increased to a lesser extent. Furthermore, more overall heat is generated by the BA/CA blends (e.g., the 50% co-fired blend (BL3) increases the cumulative heat by 5% compared to the CA mix).

Early age hydration kinetics involve many simultaneous complex processes making it difficult to link observations with specific causes. Yet inferences can be made utilizing previous research. The retarding effect caused by the ash samples may be due to the adsorption of calcium ions on the aluminum-rich ash surface resulting in the delayed nucleation and crystallization of the calcium hydroxide, calcium silicate hydrates, and ettringite.<sup>25</sup> The higher peaks associated with the finer particles in the CA and EC-series pastes may be related to an increase in available nucleation sites for hydration product formation. Kaukaouzas et al.<sup>26</sup> has shown that ash particle size decreases with increasing percentages of wood chip replacement of coal during co-firing—a trend observed with the EC ashes as well. It is possible that co-firing may increase early age heat release due to changes in particle size and morphology. The higher cumulative heat released by the coarser EC-series in comparison to the fine CA suggest that they may also possess some hydraulic properties as signified by their higher CaO contents.

On the other hand, BA presumably has no hydraulic properties (crystalline calcium aluminates were not detected during XRD) yet it still intensifies the cement hydration. Its high surface area (ten times that of CA) may initiate heterogeneous nucleation—a phenomenon shown to increase  $C_3A$  reaction at early ages.<sup>27</sup> Lagier et al.<sup>28</sup> discovered that the replacement of high-alkali cement with metakaolin—with a surface area similar to BA—resulted in a significant increase in the  $C_3A$  hydration peak. A similar occurrence could be happening here with the addition of the highly alkaline BA which may promote dissolution of aluminum (whose availability often limits calcium sulfoaluminate hydration products at early ages) from the coal ash thus intensifying the  $C_3A$  hydration. Lastly, the high absorption capacity of the BA could reduce the effective water to cement ratio, which has also been shown to increase the rate of heat evolution.<sup>29</sup>

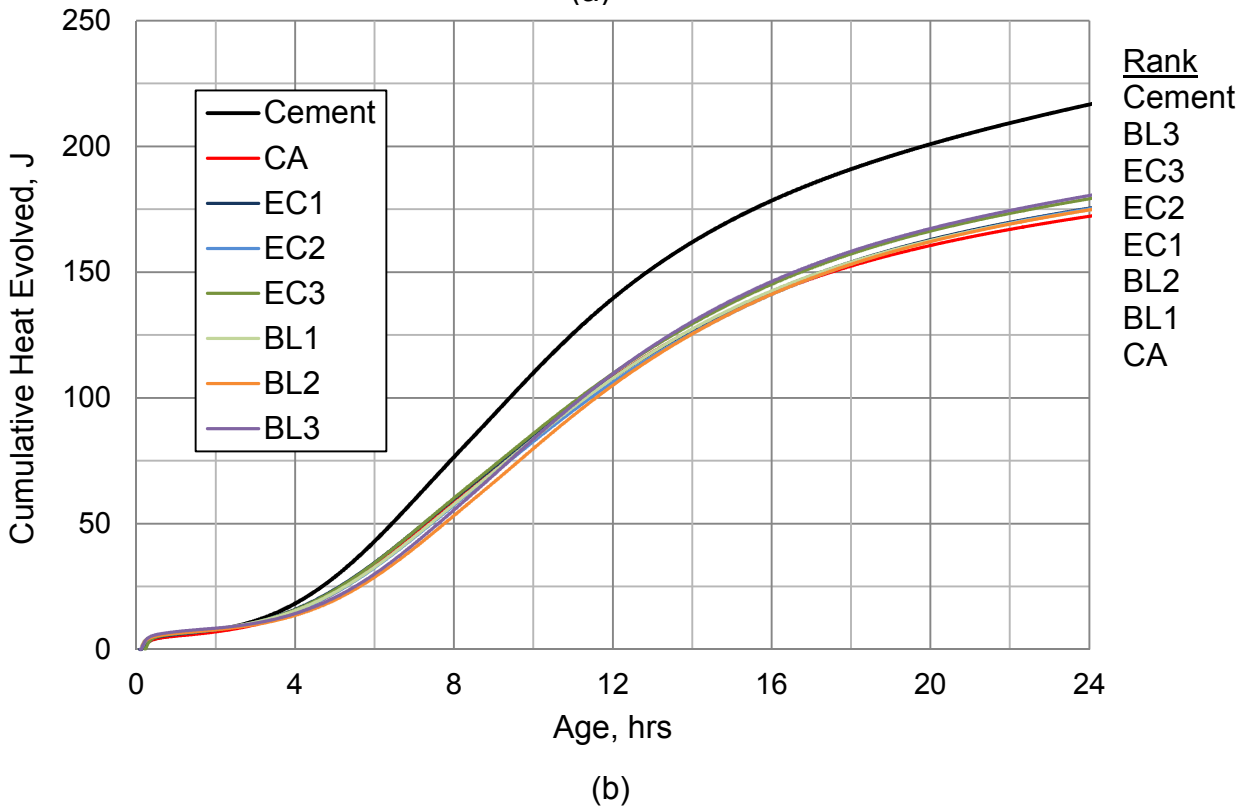
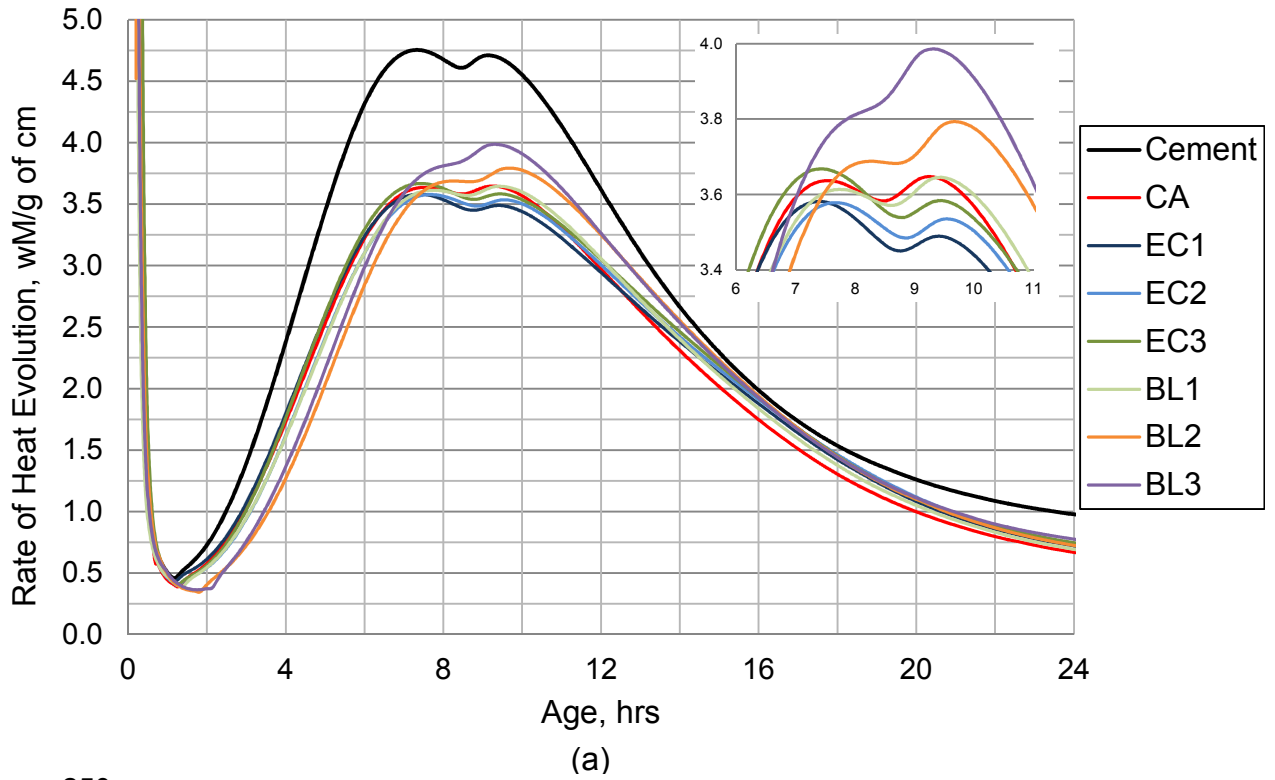


Figure 4: Isothermal calorimetry results showing the effect of ash content on (a) rate of heat evolution and (b) cumulative heat evolved per gram of cementitious materials at  $w/cm=0.40$

### *Workability*

Mortar flow results can be seen in Fig. 5. The commercial coal fly ash (CA) actually increases workability by 15% as measured by mortar flow compared to plain cement. This can be attributed to the reduction in friction in the mix due to the spherical particles—a phenomenon commonly known as the ball-bearing effect. The EC-series all significantly reduce workability by upwards of 50%. However, the ash with the highest co-fired percentage, EC3, exhibited the least reduction in workability. Therefore, it can be concluded that co-firing does not negatively impact this property for these samples. The EC3 blend mix (BL1) does not accurately represent the actual EC3 mix. The BA added to these blends has the capacity for significant moisture absorption (research is currently being performed to quantify this value). Since the BA was oven-dried to maintain consistent results between mixes, the water demand of the blends increases with increasing addition of the BA ash as evidenced by the subsequent reduction in mortar flow. Moreover the percentage reduction in mortar flow is greater than the percentage addition of BA. Yet the resulting mortar flows for these blends are still high in comparison to the cement-only mix indicating the positive CA ash properties outweigh the negative properties of the BA ash with respect to workability.

Rheological behavior in ash-cement mixtures is strongly influenced by shape morphology, fineness, loss on ignition, water demand, and particle distribution of the ash among other factors.<sup>30</sup> The higher LOI of the EC-series (and the corresponding water demand associated with increased carbon content) is likely one reason for its reduced workability. Furthermore, Mora et al.<sup>31</sup> concluded that flow spread decreased with increasing mean diameter of the ash particle. The EC-series are much coarser than the CA sample resulting in the reduced flow. The cause of the variability observed within the EC-series is less clear. The angular morphology of the wood ash particle observed under SEM in the co-fired mix should decrease workability, however this did not occur. It appears other factors (i.e., smaller particle size and reduced LOI) are more dominant. Similarly, it should be noted that the LOI of the EC3 blend mix does not accurately represent that of the EC3 sample, which could be another reason for the observed disparity. More research on the effect biomass particle morphology and water absorption has on workability is needed to clarify these issues.

### *Setting*

Initial and final setting times of the cement and blended pastes as measured by the Vicat apparatus can be seen in Fig. 6. Initial set is essentially the point beyond which the concrete has become unworkable (i.e., difficult to pour and finish). Final set occurs when there is a complete loss of plasticity in the paste. Final setting times for the plain cement, CA, and EC-series were all at 6.25 hours. Initial setting times were nearly identical for CA and the EC-series mixes compared to the plain cement paste as well. All three blends lengthened initial set by 0.75-1 hours and final set by 0.25-0.5 hours compared to the plain cement paste. The early stiffening behavior is controlled by the gradual loss of free water in the cement paste as hydration products are formed.<sup>32</sup> Thus a delay in setting time is typically observed for fly ash mixes due to less initial hydration.<sup>33</sup> However, this phenomenon was not observed for these samples as setting time was not significantly affected by the ash addition.

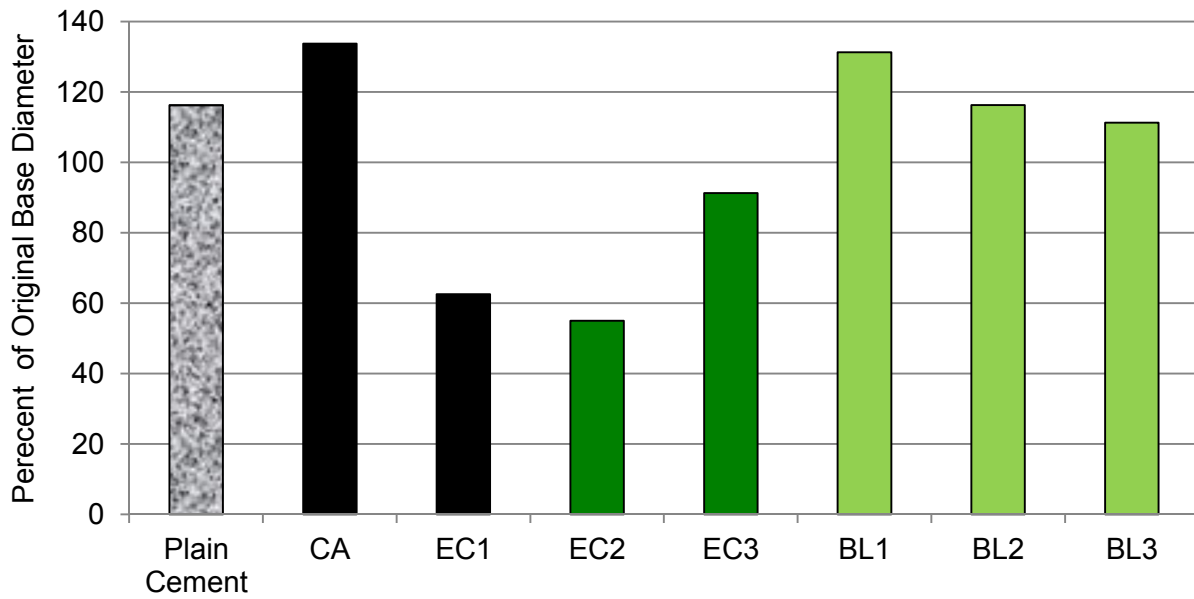


Figure 5: Mortar flow of ash mixes

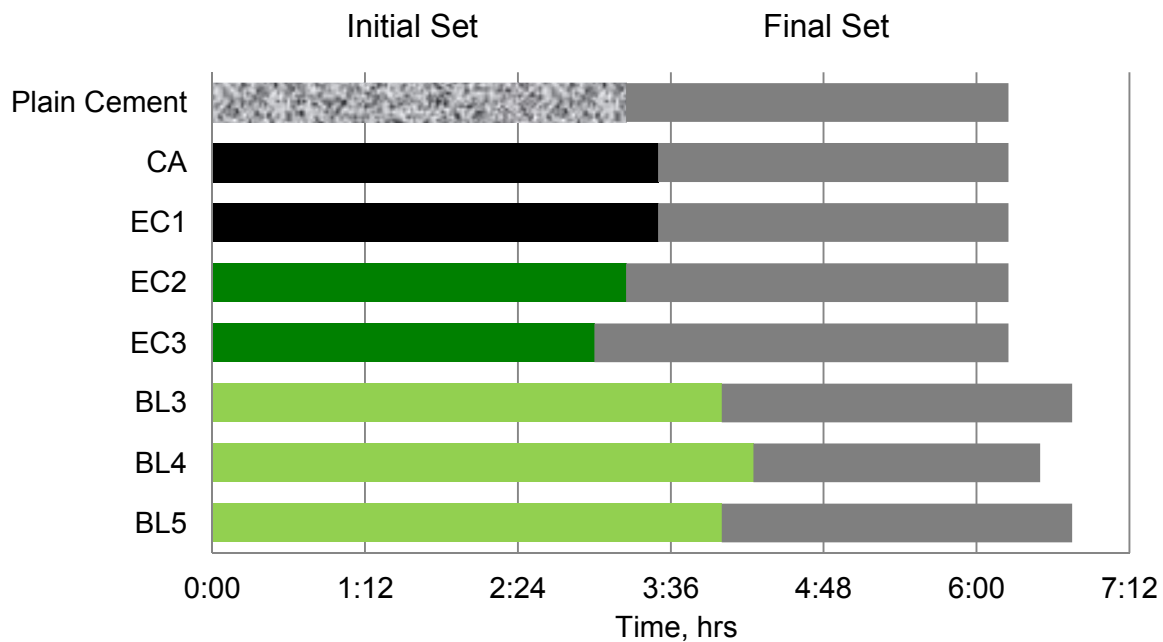


Figure 6: Setting time of ash mixes

## CONCLUSIONS

This study evaluated the performance of biomass and co-fired fly ash used in concrete by assessing its effect on early age behavior. No correlation was observed between increased co-firing percentages and increased LOI or alkali content of the ash. Yet microscopy reveals that co-firing does impact ash morphology. All ash samples reduced the heat generated during early hydration compared to cement, as expected. There

appears to be a correlation between finer ash and an increase in the C<sub>3</sub>A peak. Furthermore, co-firing resulted in finer particles which increased cumulative heat presumably due to the nucleation effect. Biomass ash significantly impacts the calorimetry curves primarily by retarding the induction period and intensifying ettringite formation. Possible reasons for this include heterogeneous nucleation due to its high surface area, increased available aluminum due to its high alkali content, and reduction in free water due to its high absorption capacity. Workability of the mixes was detrimentally affected by ash with high carbon content, high water demand, and non-spherical morphology. However, co-firing did not seem to impact mortar flow for these samples. Setting time was not meaningfully changed by the addition of ash. The blend of the coal and biomass fly ash did not accurately represent the EC3 co-fired ash in terms of these measured properties. The combustion conditions during co-firing with coal may have produced wood ash properties in the co-fired ash that were different from those in ash derived from pure biomass combustion for this sample. Furthermore, the biomass source of these two samples differed which could result in dissimilar physical and chemical ash characteristics. However, it cannot be concluded from this study that blends of other sources of coal and biomass fly ash do not represent a corresponding co-fired ash sample. Overall, this preliminary research demonstrates that further analysis is necessary to assess the impact of this emerging class of energy by-products on concrete performance before they become a viable supplementary cementitious material.

## ACKNOWLEDGMENTS

This research was supported in part by an award from the Department of Energy (DOE) Office of Science Graduate Fellowship Program (DOE SCGF). The DOE SCGF Program was made possible in part by the American Recovery and Reinvestment Act of 2009. The DOE SCGF program is administered by the Oak Ridge Institute for Science and Education for the DOE. ORISE is managed by Oak Ridge Associated Universities (ORAU) under DOE contract number DE-AC05-06OR23100. All opinions expressed in this paper are the author's and do not necessarily reflect the policies and views of DOE, ORAU, or ORISE.

## REFERENCES

- [1] American Coal Ash Association, 2009 Coal Combustion Product (CCP) Production & Use Survey Report, ACAA, Aurora, CO, < [http://www.acaa-usa.org/associations/8003/files/2009\\_Production\\_and\\_Use\\_Survey\\_Goss\\_FINAL\\_110310.pdf](http://www.acaa-usa.org/associations/8003/files/2009_Production_and_Use_Survey_Goss_FINAL_110310.pdf)>.
- [2] Baxter, L. Biomass-coal co-combustion: opportunity for affordable renewable energy, *Fuel*, 2005, 84, pp. 1295-1302.
- [3] Maciejewska, A., Veringa, H., Sanders, J., and Peteves, S. D. Co-firing of biomass with coal: Constraints and role of biomass pre-treatment, DG-JRC Institute for Energy,

2006, <[http://ie.jrc.ec.europa.eu/publications/scientific\\_publications/2006/EUR22461EN.pdf](http://ie.jrc.ec.europa.eu/publications/scientific_publications/2006/EUR22461EN.pdf)>.

[4] Thomas, M. Effect of SCMs on the hardened properties of concrete, PCA, University of New Brunswick, 2006.

[5] Standard Specification for Fly Ash and Raw or Calcined Natural Pozzolan for Use in Concrete, ASTM C 618, American Society for Testing and Materials, West Conshohocken, PA, 2008.

[6] Naik, T.R., Rudolph, N.K., and Siddique, R. Controlled Low-Strength Materials Containing Mixtures of Coal Ash and New Pozzolanic Material, ACI Materials Journal, 2003, 100(3), pp. 208-215.

[7] Wang, S. and Baxter, L. Comprehensive study of biomass fly ash in concrete: Strength, microscopy, kinetics, and durability, Fuel, 2007, 88, pp. 1165-1170.

[8] Wang, S., Llamazos, E., Baxter, L., and Fonseca, F. Durability of biomass fly ash in concrete: Freezing and thawing and rapid chloride permeability tests, Fuel, 2008, 87, pp. 359-364.

[9] Wang, S., Miller, A., Baxter, L., and Fonseca, F. Biomass fly ash in concrete: SEM, EDX and ESEM analysis, Fuel, 2008, 87, pp. 372-379.

[10] Wang, S., Miller, A., Llamazos, E., Fonseca, F., and Baxter, L. Biomass fly ash in concrete: Mixture proportioning and mechanical properties, Fuel, 2008, 87, pp. 363-371.

[11] Dockter, B.A. and Eylands, K.E. Development of Management Options for Biomass Combustion By-Products. International Ash Symposium, University of Kentucky, Oct. 20-22, 2003.

[12] Fly ash for concrete - Part 1: Definition, specifications and conformity criteria, EN-450, European Standard, Brussels, Belgium, 2005.

[13] Standard Specification for Portland Cement, ASTM C 150, American Society for Testing and Materials, West Conshohocken, PA, 2009.

[14] Loo, S. van and Koppejan, J. The Handbook of Biomass Combustion & Co-Firing, Earthscan, 2008.

[15] Demirbas, A. Sustainable cofiring of biomass with coal, Energy Conversion and Management, 2003, 44, pp. 1465-1479.

[16] Saraber, A.J. and Berg, J.W. van den, How to understand effects of co-combustion on fly ash quality? Technical aspects. In the Proceedings of AshTech, Birmingham, UK, May 14-17, 2006.

- [17] Mahendra, M.K., Ragland, K.W., and Baker A.J. Wood ash composition as a function of furnace temperature, *Biomass and Bioenergy*, 1993, 4(2), pp. 103-116.
- [18] Standard Practice for Measuring Hydration Kinetics of Hydraulic Cementitious Mixtures Using Isothermal Calorimetry, ASTM C 1679, American Society for Testing and Materials, West Conshohocken, PA, 2008.
- [19] Garas, V.Y. and Kurtis, K.E. Assessment of methods for optimising ternary blended concrete containing metakaolin, *Magazine of Concrete Research*, 2008, 60(7), pp. 499-510.
- [20] Standard Test Method for Compressive Strength of Hydraulic Cement Mortars, ASTM C 109, American Society for Testing and Materials, West Conshohocken, PA, 2008.
- [21] Standard Specification for Standard Sand, ASTM C 778, American Society for Testing and Materials, West Conshohocken, PA, 2006.
- [22] Standard Practice for Mechanical Mixing of Hydraulic Cement Pastes and Mortars of Plastic Consistency, ASTM C 305, American Society for Testing and Materials, West Conshohocken, PA, 2006.
- [23] Standard Test Method for Flow of Hydraulic Cement Mortar, ASTM C 1437, American Society for Testing and Materials, West Conshohocken, PA, 2007.
- [24] Standard Test Methods for Time of Setting of Hydraulic Cement by Vicat Needle, ASTM C 191, American Society for Testing and Materials, West Conshohocken, PA, 2008.
- [25] Wei, F.F., Grutzeck, M.W., and Roy, D.M. The retarding effects of fly ash upon the hydration of cement pastes: The first 24 hours, *Cement and Concrete Research*, 1985, 15, pp. 174–184.
- [26] Koukouzas, N., Hämäläinen, J., Ketikidis, C., Papanikolaou, D., and Tremouli, A. Definition of mineral and chemical composition of fly ash derived from CFB combustion of coal with biomass. *World of Coal Ash (WOCA)*, Covington, Kentucky, May 7-10, 2007.
- [27] Jayapalan, A.R., Lee, B.Y., Fredrich, S. M., and Kurtis, K.E. Influence of Additions of Anatase TiO<sub>2</sub> Nanoparticles on Early-Age Properties of Cement-Based Materials, *Transportation Research Record: Journal of the Transportation Research Board*, 2010, No. 2141, pp. 41-46.

- [28] Lagier, F. and Kurtis, K.E. Influence of Portland cement composition on early age reactions with metakaolin, *Cement and Concrete Research*, 2007, 37(10), pp. 1411-1417.
- [29] Johansen, N.A., Millard, M.J., Mezencevova, A., Garas, V.Y., and Kurtis, K.E. New method for determination of absorption capacity of internal curing agents, *Cement and Concrete Research*, 2009, 39, pp. 65-68.
- [30] Payá, J., Monzó, J., Borrachero, M.V., Mora, E.P., and González-López, E. Mechanical treatment of fly ashes Part II: Particle morphologies in ground fly ashes (GFA) and workability of GFA-cement mortars, *Cement and Concrete Research*, 26(2), 1996, pp. 225-235.
- [31] Mora, E.P., Payá, J., and Monzó, J. Influence of different sized fractions of a fly ash on workability of mortars, *Cement and Concrete Research*, 1993, 23, pp. 917-924.
- [32] Mehta, P.K. and Monteiro, P.J.M., *Concrete: Microstructure, Properties, and Materials*, McGraw-Hill Professional, New York, NY, 2005.
- [33] Bentz, D.P. and Ferraris C.F. Rheology and setting of high volume fly ash mixtures, *Cement & Concrete Composites*, 2010, 32, pp. 265-270.